

Absolute intensity normalisation of powder neutron scattering data

Joseph A. M. Paddison^{1,*}

¹*Neutron Scattering Division, Oak Ridge National Laboratory, Oak Ridge, Tennessee 37831, USA*

An important property of neutron scattering data is that they can be normalised in absolute intensity units. In practice, however, such normalisation is often not performed, since it can be time-consuming and subject to systematic uncertainties. Here, a straightforward approach is presented for absolute intensity normalisation of neutron scattering data from polycrystalline samples. This approach uses the intensity scale factor obtained from a Rietveld refinement to normalise the data to the nuclear Bragg profile of the sample. Factors to convert the Rietveld scale factor into an absolute normalisation factor are tabulated for constant-wavelength and time-of-flight data refined using the popular programs Fullprof and GSAS-II. An example of the application of this method to experimental data is presented. Advantages, disadvantages, and extensions of this approach to spectroscopic data are discussed.

INTRODUCTION

Among crystallographic measurements, neutron scattering has the useful and unique property that the measured scattering profile can be placed on an absolute intensity scale. This property is important in the study of disordered crystalline materials using total scattering or pair-distribution function (PDF) techniques [1, 2], where it enables accurate measurement of coordination numbers, and can be necessary to use modelling approaches such as reverse Monte Carlo refinement [3, 4]. It is also important in magnetic neutron scattering, since it allows for quantitative determination the magnitude of ordered magnetic moments, diffuse scattering, and excitations [5, 6]. This information cannot typically be obtained from other techniques such as resonant X-ray scattering, and is relevant to scientific problems of ongoing importance, such as the question of the “missing” magnetic spectral weight in high- T_c superconductors [7] and the “quantumness” of the magnetic excitations of quantum magnets [8].

Despite the value of absolute intensity measurements, most published neutron scattering patterns only report the intensity in relative units (e.g., counts per unit time) rather than absolute units (e.g., barn sr⁻¹ atom⁻¹). A likely explanation is that current approaches to data normalisation present some practical difficulties. For example, a common approach is to normalise data to the incoherent scattering from a separately-measured vanadium calibration sample [9, 10]. This method requires accurate measurement of the vanadium standard, the packing fraction of the sample, the mass of vanadium in the beam, and the absorption of the sample and the vanadium, which can be time-consuming [10, 11]. An alternative approach is to normalise the data to the incoherent scattering from the sample itself [10]. This difficulty here is that extraneous effects – background scattering from the apparatus, diffuse scattering from chemical short-range ordering in the sample, and additional incoherent scattering from any hydrogen-containing impurities – will add to the apparent incoherent scattering, giving a systematic uncertainty that is difficult to quantify [10].

In this short communication, I present an alternative approach to absolute normalisation of neutron scattering data for polycrystalline materials: normalisation to the nuclear Bragg

profile of the sample itself. The nuclear Bragg profile is routinely calculated in widely-used software for Rietveld refinement [12], such as Fullprof [13, 14], GSAS-II [15], and Topas [16]. This calculation can be done in absolute intensity units for any material with a known crystal structure, since the relevant scattering equations and scattering lengths are known [17]. Unfortunately, however, Rietveld programs do *not* calculate the nuclear Bragg profile in absolute intensity units, so the intensity scale factor obtained from a Rietveld refinement cannot be applied directly to normalise the data. The main result of this paper is a set of simple formulae (see Table I) that convert the Rietveld scale factor into an “absolute normalisation factor” that transforms the data into absolute intensity units. Using this approach, scattering data from polycrystalline materials can be normalised with little effort beyond a Rietveld refinement.

This paper is structured as follows. I start with a derivation of the relationship between the absolute normalisation factor and the Rietveld scale factor. I then provide an example using published experimental data for the frustrated magnet Dy₃Mg₂Sb₃O₁₄ [18]. To demonstrate the accuracy and reproducibility of the method, results are compared for constant-wavelength and time-of-flight data measured on the same material. I conclude by summarising the key results and providing a table of absolute normalisation factors for the common Rietveld programs Fullprof and GSAS-II. A reader who is interested in applying the approach can skip the derivations and refer to Table I.

DERIVATION

I start by assuming that the nuclear profile intensity measured experimentally, I_{expt} , is proportional to the absolute nuclear intensity in units of barn sr⁻¹ atom⁻¹:

$$I_{\text{expt}} = sI_{\text{abs}}. \quad (1)$$

Our aim is to find the proportionality constant s . We call the overall intensity scale factor obtained from Rietveld refinement `RietveldScale`. This parameter multiplies the intensity I_0 calculated internally by the Rietveld refinement program, so that after the refinement has converged, the result

optimally matches the experimental data:

$$I_{\text{expt}} = \text{RietveldScale} \times I_0. \quad (2)$$

It follows that

$$s = \text{RietveldScale} \times \frac{I_0}{I_{\text{abs}}}. \quad (3)$$

Hence, to determine s , we require expressions for both I_0 and I_{abs} . These are given below.

The general equation for the Q -dependence of the Bragg scattering intensity for a polycrystalline sample is given by [19]

$$I_{\text{abs}}(Q) = \frac{2\pi^2}{NV} \sum_{\mathbf{G}} \frac{m_{\mathbf{G}} |F_{\mathbf{G}}|^2}{G^2} R_Q(Q - G), \quad (4)$$

where V is the volume of the crystallographic unit cell containing N atoms, \mathbf{G} labels a set of equivalent Bragg reflections having multiplicity $m_{\mathbf{G}}$, $G = |\mathbf{G}|$ is the length of a reciprocal-lattice vector, $R_Q(Q - G)$ is a resolution function that obeys the normalisation condition $\int R_Q(Q - G) dQ = 1$, and the structure factor

$$F_{\mathbf{G}} = \sum_{j=1}^N b_j T_j \exp(i\mathbf{G} \cdot \mathbf{r}_j), \quad (5)$$

where \mathbf{r}_j is the position of atom j in the unit cell, b_j is its nuclear scattering length (in units of 10^{-12} cm), T_j is its Debye-Waller factor, and the sum is taken over all N atoms in the unit cell [19]. Eq. (4) gives the intensity in absolute units of $\text{barn sr}^{-1} \text{atom}^{-1}$.

The profile intensity calculated internally in Rietveld refinement depends on the Rietveld program. In the derivation below, I will use FullProf [14] as an example; the results for GSAS-II are different and given in Table I. The profile intensity calculated internally by FullProf is given by

$$I_0(x) = \sum_{\mathbf{G}} m_{\mathbf{G}} |F_{\mathbf{G}}|^2 L_x R_x(x - x_{\mathbf{G}}), \quad (6)$$

where x denotes either scattering angle 2θ for constant-wavelength diffraction or time t for time-of-flight diffraction, and $R_x(x - x_{\mathbf{G}})$ is a resolution function that again obeys $\int R_x(x - x_{\mathbf{G}}) dx = 1$. The expressions for Lorentz factor L_x and resolution function are written with subscript x to emphasise that they differ for time-of-flight vs. constant-wavelength data. I note that Eq. (6) assumes that the data have already been corrected for absorption (and any other relevant corrections to the overall intensity) before being used as input for Rietveld refinement.

Constant-wavelength diffraction

To compare the equations for I_0 and I_{abs} , it is necessary to change the variable from Q to scattering angle. For constant-wavelength diffraction, this conversion is

$$Q = \frac{4\pi \sin \theta}{\lambda}, \quad (7)$$

where λ is the fixed incident neutron wavelength in Å, and 2θ is scattering angle in degrees. The change-of-variable rule gives

$$R_Q(Q - G) = \left| \frac{d(2\theta)}{dQ} \right| R_{2\theta}(2\theta - 2\theta_{\mathbf{G}}) \quad (8)$$

$$= \frac{90\lambda}{\pi^2 \cos \theta_{\mathbf{G}}} R_{2\theta}(2\theta - 2\theta_{\mathbf{G}}). \quad (9)$$

It follows from Eqs. (4) and (9) that the absolute scattering intensity (in $\text{barn sr}^{-1} \text{atom}^{-1}$) is given by

$$I_{\text{abs}}(2\theta) = \frac{45\lambda^3}{2\pi^2 NV} \sum_{\mathbf{G}} m_{\mathbf{G}} |F_{\mathbf{G}}|^2 L_{2\theta} R_{2\theta}(2\theta - 2\theta_{\mathbf{G}}), \quad (10)$$

where the geometrical factors have been combined into the Lorentz factor for constant-wavelength diffraction,

$$L_{2\theta} \equiv \frac{1}{2 \sin^2 \theta_{\mathbf{G}} \cos \theta_{\mathbf{G}}}. \quad (11)$$

Hence, from Eqs. (3), (6) and (10), we obtain the absolute normalisation factor for FullProf,

$$s_{2\theta}^{\text{Fullprof}} = \text{FullprofScale} \times \frac{2\pi^2 NV}{45\lambda^3}. \quad (12)$$

The result for GSAS-II differs because its intensity calculation divides Eq. (6) by V , and uses units of centidegrees for scattering angle [20]. Following the steps above, we obtain

$$s_{2\theta}^{\text{GSAS}} = \text{GSASScale} \times \frac{2\pi^2 N}{4500\lambda^3}. \quad (13)$$

To obtain the absolute scattering intensity, simply divide the experimental profile by the relevant $s_{2\theta}$ for FullProf or GSAS-II.

Time-of-flight diffraction

For time-of-flight diffraction, the relationship between Q and t is

$$Q = \frac{4\pi m_n l \sin \theta}{ht}, \quad (14)$$

which is obtained from Eq. (7) by applying the de Broglie relation, $\lambda = ht/m_n l$, where t is time of flight, l is total neutron path length, and m_n is neutron mass. In time-of-flight diffraction, l and the scattering angle 2θ are fixed for a particular detector bank. Applying the change-of-variable rule,

$$R_Q(Q - G) = \left| \frac{dt}{dQ} \right| R_t(t - t_{\mathbf{G}}) \quad (15)$$

$$= \frac{4\pi m_n l \sin \theta}{hG^2} R_t(t - t_{\mathbf{G}}). \quad (16)$$

It follows from Eqs. (4) and (16) that the absolute intensity is given by

$$I_{\text{abs}}(t) = \frac{m_n l}{2\pi h NV} \sum_{\mathbf{G}} m_{\mathbf{G}} |F_{\mathbf{G}}|^2 L_t R_t(t - t_{\mathbf{G}}), \quad (17)$$

	Fullprof	GSAS-II
Constant wavelength	$\text{FullprofScale} \times \frac{2\pi^2 NV}{45\lambda^3}$	$\text{GSASScale} \times \frac{2\pi^2 N}{4500\lambda^3}$
Time of flight	$\text{FullprofScale} \times \frac{4\pi NV \sin \theta}{\text{dtt1}} (*)$	$\text{GSASScale} \times \frac{4\pi N \sin \theta}{\text{DIFC}}$

TABLE I. Factors to convert measured intensity profile to absolute intensity units. **To convert data into absolute intensity units of barnsr⁻¹atom⁻¹, divide the measured intensity profile by the relevant number obtained from this table.** FullprofScale is the intensity scale factor refined using FullProf, GSASScale is the intensity scale factor refined using GSAS-II, V is the volume of the unit cell in Å³, and N is the number of atoms in the unit cell. For constant-wavelength data, λ is the neutron wavelength in Å. For time-of-flight data, θ is the constant scattering angle of the detector bank, and dtt1 or DIFC is the diffractometer constant with units of $\mu\text{s}\text{Å}^{-1}$ that relates d -spacing (in Å) to time-of-flight (in μs). Note that N here denotes the total number of atoms per unit cell, so absolute intensity will be in barnsr⁻¹atom⁻¹. To normalise to the number of magnetic atoms, replace N by the number of magnetic atoms per unit cell.

Important note: The correction factors in this table assume that the Rietveld program does not apply overall intensity corrections for experimental effects such as absorption. If such corrections are needed, they should be applied directly to the data prior to the Rietveld refinement. (*) Note: For some formats of time-of-flight data, such as multi-bank data in RAL format, FullProf internally multiplies the data by a factor of 1000. In such cases, this conversion factor should be replaced by $\text{FullprofScale} \times 0.001 \times \frac{4\pi NV \sin \theta}{\text{dtt1}}$ when applied to the original data.

where the geometrical factors have been combined into the Lorentz factor for time-of-flight diffraction [21],

$$L_t \equiv d^4 \sin \theta, \quad (18)$$

where $d = 2\pi/G$ is the d -spacing of the Bragg reflection. This yields for the absolute normalisation factor

$$s_t^{\text{Fullprof}} = \text{FullprofScale} \times \frac{4\pi NV \sin \theta}{\text{DIFC}}, \quad (19)$$

where

$$\text{DIFC} = \frac{2m_n l \sin \theta}{h} \quad (20)$$

is an instrument parameter (also called dtt1 in FullProf), which has units of $\mu\text{s}\text{Å}^{-1}$ and relates d -spacing in Å to time-of-flight in μs . For GSAS, the result is

$$s_t^{\text{GSAS}} = \text{GSASScale} \times \frac{4\pi N \sin \theta}{\text{DIFC}}. \quad (21)$$

Again, to obtain the absolute scattering intensity, simply divide the experimental profile by the relevant s_t for FullProf or GSAS-II.

WORKED EXAMPLE

I now discuss an application of this method using experimental neutron-scattering data for the frustrated magnetic material Dy₃Mg₂Sb₃O₁₄, which exhibits strong magnetic diffuse scattering. These data were previously published in [18], but the normalisation was not discussed in detail. Constant-wavelength data were collected using the DCS spectrometer at NIST [22]; the data were integrated over energy and can be treated as diffraction data. Time-of-flight data were collected using the GEM diffractometer at ISIS [23].

This material crystallises in the $R\bar{3}m$ space group and the magnetic Dy atoms occupy the $9e$ site. Rietveld refinements were performed using FullProf to DCS data measured at 50 K

with $\lambda = 5 \text{ Å}$ (see [18] for details). A reasonable fit is obtained [Fig. 1(a)]. The refined unit-cell volume was 799.6(2) Å³ and the Rietveld scale factor was 0.071(1), indicating a statistical error $\sim 2\%$. Using these values in Eq. (12), we obtain $s_{2\theta}^{\text{Fullprof}} = 1.80(3)$. Rietveld refinements were also performed to GEM data measured at 25 K [Figure 1(b)], including data from banks 1 to 4 [18]. Taking bank 1 as an example, $2\theta = 9.39^\circ$ and $\text{DIFC} = 2814.83 \mu\text{s}\text{Å}^{-1}$, the refined unit-cell volume was 799.153(4) Å³, and the Rietveld scale factor was 0.00516(5). Using these values in Eq. (19), we obtain $s_t^{\text{Fullprof}} = 0.0513(5)$.

To isolate the correlated magnetic diffuse scattering, which develops at temperatures below 25 K, the 25 K or 50 K data were subtracted from low-temperature data collected at 0.5 K on each instrument. The result was divided by the appropriate s^{Fullprof} determined as above, to place both data sets into absolute units of barnsr⁻¹Dy⁻¹. For the GEM data, the different banks were also merged. The results shown in Fig. 1(c) demonstrate excellent agreement between the normalised diffuse scattering measured on GEM and DCS. This result suggests that the accuracy of this approach is likely to be significantly better than the $\sim 20\%$ systematic uncertainty that has been suggested as typical of other normalisation methods [10].

DISCUSSION AND CONCLUSIONS

I have presented a set of factors that allow neutron scattering data of polycrystalline materials to be placed on an absolute intensity scale using the Rietveld scale factor. This method offers three main advantages. First, since the nuclear scattering of the sample is used as an internal normalisation standard, no additional measurements are required. Second, systematic errors are likely to be reduced compared with approaches that use measurements of an external standard. Third, since Rietveld refinement is already an essential part of data analysis for many systems, data normalisation can be done with little extra effort.

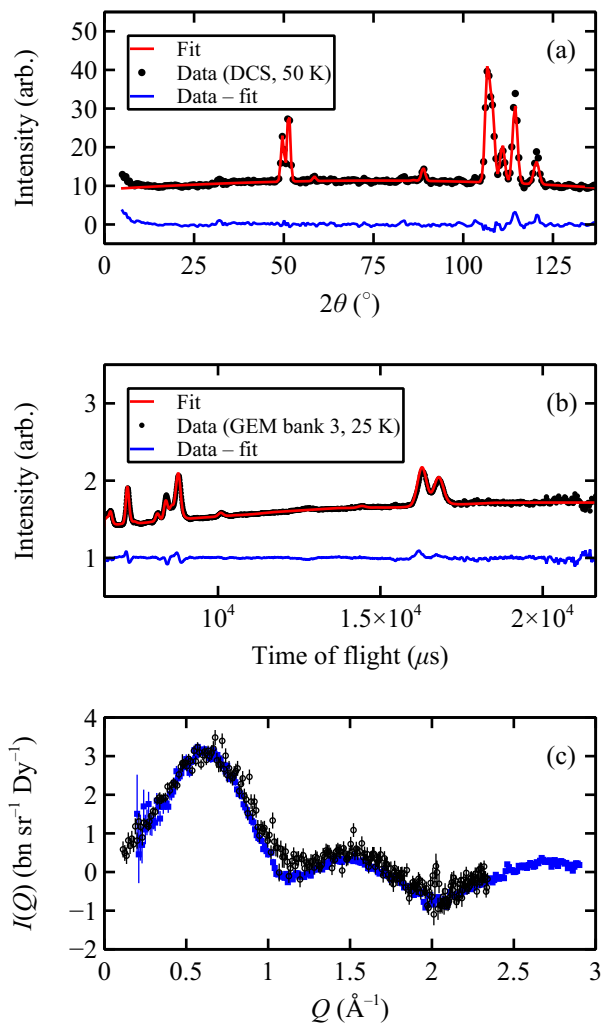


FIG. 1. (a) Nuclear refinement of constant-wavelength neutron data ($\lambda = 5 \text{ \AA}$) measured on $\text{Dy}_3\text{Mg}_2\text{Sb}_3\text{O}_{14}$ at $T = 50 \text{ K}$ using the DCS spectrometer at NIST, showing data (black circles), Rietveld fit (red line) and difference (blue line). (b) Nuclear refinement of time-of-flight neutron data measured on $\text{Dy}_3\text{Mg}_2\text{Sb}_3\text{O}_{14}$ at $T = 25 \text{ K}$ using the GEM diffractometer at ISIS, showing data (black circles), Rietveld fit (red line) and difference (blue line). (c) Magnetic diffuse scattering for $\text{Dy}_3\text{Mg}_2\text{Sb}_3\text{O}_{14}$ obtained in absolute intensity units using formulae given in Table I, showing data at $T = 0.5 \text{ K}$ measured on DCS (black circles) and GEM (blue squares). In each case, a higher-temperature data set (25 or 50 K) has been subtracted from the 0.5 K data to remove nonmagnetic scattering. Data were previously published in [18].

The main limitation of this approach is that it is not applicable to liquids, amorphous materials, or polycrystalline materials where the average structure is not well modelled using Rietveld refinement. As such, it is most useful for magnetic materials with well-ordered crystal structures, and to materials where a distinct average crystal structure coexists with short-range order. Notably, the latter class of systems includes many functional materials studied using PDF approaches [1, 24],

where both the Bragg profile and the PDF are often used to inform atomistic models [4].

The approach outlined here can also be applied to neutron spectroscopy data collected on polycrystalline samples, e.g., for measurements of phonons or magnetic excitations. In this case, data collected on direct-geometry spectrometers are binned on a grid of 2θ vs. energy transfer, integrated over the elastic energy resolution, and the energy-integrated data are used as input to a Rietveld refinement. The entire spectrum can then be normalised (in $\text{barn sr}^{-1} \text{atom}^{-1}$ per unit energy) using the factors given in Table I; some examples are discussed in [25, 26]. I therefore hope that this work will facilitate wider use of the quantitative intensity information available from neutron diffraction and spectroscopy data.

I am grateful to Stuart Calder, Danielle Yahne, and Ross Stewart for encouraging me to write this paper. Initial work was supported by the College of Sciences of Georgia Institute of Technology. Manuscript preparation was supported by the U.S. Department of Energy, Office of Science, Scientific User Facilities Division.

* paddisonja@ornl.gov

- [1] B. H. Toby, T. Egami, *Acta Crystallogr. A* **48**, 336 (1992).
- [2] S. J. L. Billinge, M. G. Kanatzidis, *Chem. Commun.* pp. 749–760 (2004).
- [3] D. A. Keen, R. L. McGreevy, *Nature* **344**, 423 (1990).
- [4] M. G. Tucker, D. A. Keen, M. T. Dove, A. L. Goodwin, Q. Hui, *J. Phys.: Condens. Matter* **19**, 335218 (2007).
- [5] K. R. A. Ziebeck, P. J. Brown, *J. Phys. F: Met. Phys.* **10**, 2015 (1980).
- [6] O. Steinsvoll, C. F. Majkrzak, G. Shirane, J. Wicksted, *Phys. Rev. B* **30**, 2377 (1984).
- [7] J. Lorenzana, G. Seibold, R. Coldea, *Phys. Rev. B* **72**, 224511 (2005).
- [8] M. Mourigal, *et al.*, *Nature Physics* **9**, 435 (2013).
- [9] G. D. Wignall, F. S. Bates, *J. Appl. Crystallogr.* **20**, 28 (1987).
- [10] G. Xu, Z. Xu, J. M. Tranquada, *Rev. Sci. Instrum.* **84**, 083906 (2013).
- [11] A. K. Soper, *GudrunN and GudrunX: programs for correcting raw neutron and X-ray diffraction data to differential scattering cross section* (Science & Technology Facilities Council Swindon, UK, 2011).
- [12] H. M. Rietveld, *J. Appl. Crystallogr.* **2**, 65 (1969).
- [13] J. Rodríguez-Carvajal, *Physica B* **192**, 55 (1993).
- [14] J. Rodríguez-Carvajal, *FullProf Manual*, Laboratoire Léon Brillouin, CEA/Saclay, 91191 Gif sur Yvette Cedex, France (2001).
- [15] B. H. Toby, R. B. Von Dreele, *J. Appl. Crystallogr.* **46**, 544 (2013).
- [16] A. A. Coelho, *J. Appl. Crystallogr.* **51**, 210 (2018).
- [17] V. F. Sears, *Neutron News* **3**, 26 (1992).
- [18] J. A. M. Paddison, *et al.*, *Nat. Commun.* **7**, 13842 (2016).
- [19] G. L. Squires, *Introduction to the Theory of Thermal Neutron Scattering* (Cambridge University Press, Cambridge, 1978).
- [20] A. C. Larson, R. B. Von Dreele, *GSAS Manual*, Los Alamos National Laboratory (1985).
- [21] Y. Zhang, J. Liu, M. G. Tucker, *Acta Crystallogr. A* **79**, 20 (2023).

- [22] J. R. D. Copley, J. C. Cook, *Chem. Phys.* **292**, 477 (2003).
[23] A. C. Hannon, *Nucl. Instrum. Methods Phys. Res. A* **551**, 88 (2005).
[24] P. F. Peterson, D. Olds, M. T. McDonnell, K. Page, *J. Appl.*

- Crystallogr.* **54**, 317 (2021).
[25] J. A. M. Paddison, *et al.*, *Cell Rep. Phys. Sci.* **5** (2024).
[26] J. A. M. Paddison, *et al.*, *npj Quantum Mater.* **9**, 48 (2024).